Use of Segmented Three-Dimensional Liver Images in Hepatectomy with a New Concept of Subsegmentation : a Step in Virtual Reality-Aided Surgery

Tetsuya Kurosaki[1], Yasuki Unemura[1], Shuichi Takahashi[2], Naoki Suzuki[3], Asaki Hattori[3], and Mitsuko Ariizumi[4]

[1]*Department of Surgery, The Jikei University School of Medicine*
[2]*Information Technology R & D Center, Mitsubishi Electric Corporation*
[3]*Institute for High Dimensional Medical Imaging,*
The Jikei University School of Medicine
[4]*Department of Radiology, The Aoyama Tokyo Metropolitan Officers' Hospital*

ABSTRACT

Although hepatectomy is usually performed by hepatobiliary surgeons, general surgeons must also understand the complicated intrahepatic relations of vessels and the vascular anatomy of liver segments so that they can perform hepatectomy safely. We constructed three-dimensional (3D) images of the interior of the liver with which segments of liver could be identified. Simulations of liver resection and various measurements were performed to examine the usefulness of reconstruction. We collected data with contrast-enhanced helical computed tomography from a healthy volunteer and a patient with cancer. The data, which were collected from venous systems, portal systems, and liver surfaces, were entered into a workstation with a high-speed operation facility and reconstructed as 3D images. Several types of hepatectomy were performed with this system. Comparison with anatomic segments showed that the system correctly indentified the portal vein and hepatic vein in liver segments and, therefore, segments could be accurately identified. Because this method allowed on-image two-point distance measurements and volume measurements of resected areas and segments, more practical preoperative simulations could be performed. Simulations of various types of hepatectomy show that this 3D system is useful for understanding the planned procedure and surgical anatomy. (Jikeikai Med J 2003 ; 50 : 59-68)

Key words : three-dimensional imaging, virtual reality-assisted surgery, liver simulation surgery, real-time simulation

INTRODUCTION

Hepatectomy has recently been performed more often to treat liver tumors because of improvements in preoperative diagnosis, operative techniques, and postoperative care[1-3]. However, hepatectomy is still performed mostly by hepatobiliary surgeons, perhaps because of the belief that specialized training is needed to understand the anatomy of the liver. For he-

patectomy to be performed safely and effectively, the surgeon must recognize the incurrent blood vessels, the veins draining the cancer-bearing areas, and the structure of liver segments. However, general surgeons often have difficulty understanding these three-dimensional (3D) relationships with preoperative two-dimensional images because the intrahepatic vessels — Glisson's system and the venous system — intersect in an extremely complicated way. A better under-

standing of 3D relationships would enable general surgeons to perform hepatectomy with greater safety and less difficulty.

Recently, the use of 3D imaging in surgery has increased[4-11]. In hepatic surgery, 3D imaging allows intrahepatic vessels to be visualized[4,5] and has been used for preoperative diagnosis[6,7], operative planning[8,9], puncture simulations[10], and regeneration simulations of the postoperative liver[8,9]. Although such 3D images aid visual understanding, most show only limited anatomic areas and can be examined in only certain locations, such as outside the operating room.

With a goal of developing virtual reality-aided surgery so that both hepatic surgeons and general surgeons can perform hepatectomy more safely and effectively, we have developed a system that allows 3D images to be viewed during hepatectomy[8,9,12-14]. In this study, we used an improved version of our system to project segmental borders onto the surface of the liver. We also used this system to simulate several types of hepatectomy.

Methods

3D image reconstruction

The two-dimensional images that were used to reconstruct 3D images were obtained from a healthy volunteer and a patient with liver cancer. In both subjects, the data were collected with contrast-enhanced helical computed tomography (CT) (Somatom Plus 4, Siemens Medical Systems, Erlangen, Germany). In the healthy volunteer, 100 ml of iopamidol was infused at 3 ml/second into the cubital vein. Scanning was started 20 seconds after the end of infusion. Under these conditions, only the portal vein is enhanced, allowing Glisson's system and the venous system to be easily distinguished. Scanning produced 183 2-mm-thick slices, which were reconstructed at 1-mm intervals. In the patient with cancer, scanning produced 4-mm-thick slices,which were reconstructed at 2-mm intervals. The data were entered into a personal computer (Macintosh, Power PC, 180-MHz microprocessor, 80 MB of random access memory, Apple Computer, Cupertino, CA), arranged for thresholds and contrasts with Adobe Photoshop 4.0 (Adobe

Systems, San Jose, CA) and processed semiautomatically to delete noise. The data were manually extracted to separate the venous system, Glisson's system, and the liver surface. The sampled data were translated to slice data of 512×512 pixels with a 256-level gray scale. Then, the data were entered into a workstation with a high-speed operation facility (Indigo, 512 MB of random access memory, Silicon Graphics Inc., Mountain View, CA) and reconstructed into 3D images of the hepatic surfaces, the venous systems, and Glisson's systems with voxels of $0.5 \times 0.5 \times 1.0$ mm. The reconstructed 3D images were placed in a virtual space with the same coordinate axis. Because data of the three different structures (venous system, Glisson's system, and liver surface) were extracted from the same slices, there was no dissociation in the 3D space between the structures. This enabled each of the constituent voxels to be recognized at its own coordinate in 3D space.

Image display

To display 3D images, we used the wire-frame method (Fig. 1A, B, C) and a volume-rendering method (Fig. 1D). In the wire-frame method, we showed data of every second sampled slice to decrease the information load and allow real-time expansion, reduction, rotation, and border generation. The simulation results can also be shown with the volume-rendering method. The points on the image were also designated during simulation in the volume-rendering method.

Dividing liver segments

Based on Couinaud's segmentation[15], we divided liver segments according to portal venous branches. First, the left and right hepatic lobes were divided with Cantlie's line. Then, the anterior and posterior segments were divided by a plane defined by two optional points on the right hepatic vein and one point on the bifurcation of the anterior and posterior segments of the portal vein. The borders of the medial and lateral segments were determined with the umbilical portion of the portal vein.
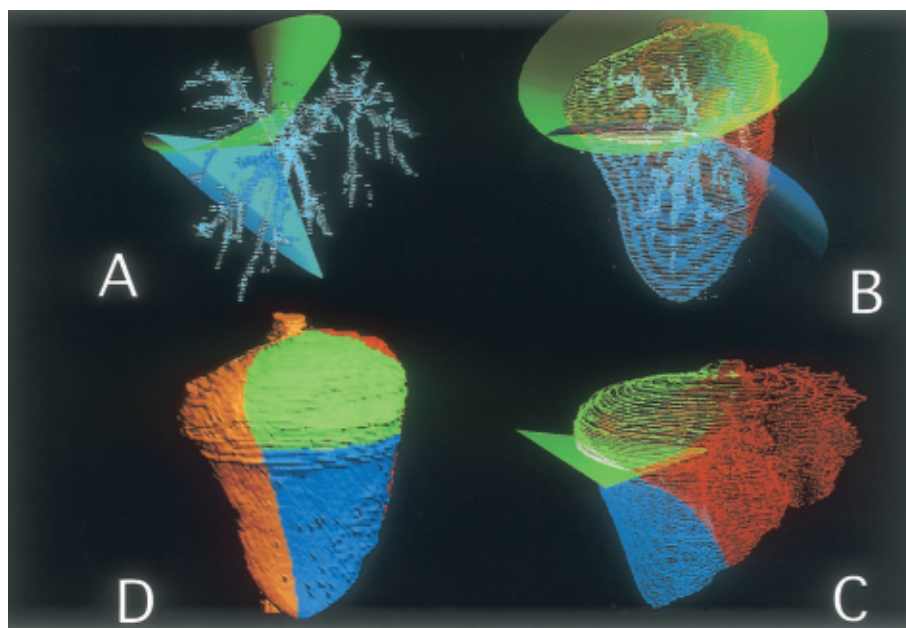
Fig. 1. Cephalocaudal subsegment interface.   The interface of subsegments S5 and S8 is defined by procedures A to D.   A : Generation of cone.   B : Projection of the base of the cone to the liver surface.   C : Setting the interface dividing the common area equally.   D : Subsegmentation in volume–rendering model.

On the borders between cephalocaudal segments, such as S5 and S8, S6 and S7, and S2 and S3, no structures, such as the hepatic vein, can be used as landmarks.   Therefore, for convenience, we decided to express an area in which a portal venous branch was dominant as a cone around the branch.   Because tertiary and more–peripheral branches of the portal vein normally dominate liver segments, we generated a cone with its apex at the third bifurcation of the portal vein and assumed that all branches distal to the third branch were within the cone. We further assumed that an interface existed which divided the area of overlap between two cones into halves.

The following procedures were performed :

1.   At every vessel bifurcation, we assumed a cone was present along each vessel with its apex at the bifurcation (Fig. 1A).   The base of the cone was projected onto the hepatic surface (Fig. 1B).

2.   Planes defined by three points were generated.   Two of the three points are where the circumferences of the areas projected on the hepatic surface intersect, and the third point is on the bifurcation of the blood vessel (Fig. 1C).

3.   The plane was set as an interface of areas where each blood vessel was dominant (Fig. 1C, D).

The angle at the apex of the cone can be adjusted freely.

Procedure for dividing segments 5 and 8

Fig. 1A shows the cones generated from the bifurcation of the portal veins of segments S5 and S8.   The angles and the bases of the cones were expanded until the cones overlapped.   The cones were then projected onto the hepatic surface (Fig. 1B).   Two points were determined which equally divided the overlapping area of two projections on the liver surface.   A plane defined by a point at the portal vein bifurcation and these two points (Fig. 1C) was generated and established as the interface of segments S5 and S8 (Fig. 1D). We used this method to determine segments for other areas, except S1 (Fig. 2).

Verification of blood vessel system

We observed the peripheral portal and hepatic vein branches of the segments determined with this system and verified that the segments were divided anatomically according to the dominant blood vessel.
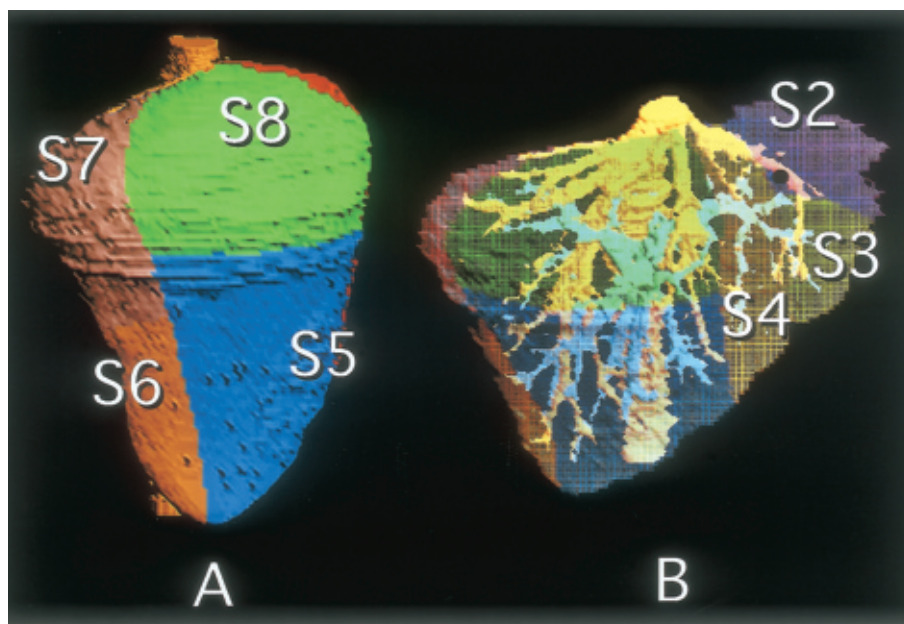
Fig. 2. 3D image of the entire liver divided into subsegments by the system. A : Lateral view : right lobe. B : Anterior view : left and right lobes. Observation is possible from any direction.

We created a function to change the color of blood vessels only within designated segments and confirmed this verification.

Simulation of hepatectomy

We simulated several hepatectomies to investigate how to apply this system of liver segmentation to actual hepatectomies. First, we used 3D images from the healthy volunteer to plan resection of segment S8. We attempted to display the smaller segment and planned the smaller resection with the cone-generation method that we had used to determine the segment borders. We resected a small segment corresponding to a 20-mm-diameter tumor in segment S7.

We also simulated a S6 resection with 3D images obtained from the patient with cancer. We investigated the validity of the surgical plan by measuring the assumed resected specimen.

RESULTS

Observation of the completed model

The completed 3D model can be observed from any angle. The direction of observation can be chan-

ged in real time in the wire-frame method but not in the volume-rendering method. However, the displays of the two methods are interlocked, so that the image can be displayed in the volume-rendering method at the same angle as determined with the wire- frame method. Also, any combination of displays of the liver parenchyma, Glisson's system, and venous system can be shown at the same time (Fig. 2B).

Segment display

By observing images divided into segments, the size of each part can be recognized intuitively (Fig. 2). In the healthy volunteer, segment S5 can easily be recognized as being abnormally large and S6 as abnormally small. Furthermore, this system can be used to measure actual volumes by calculating the constituent voxels of the segment. This function allowed us to objectively determine the size of each segment (Fig. 3).

Distribution of blood vessels in segments

Both the portal vein branch that flows into divided segments and the hepatic vein branch that
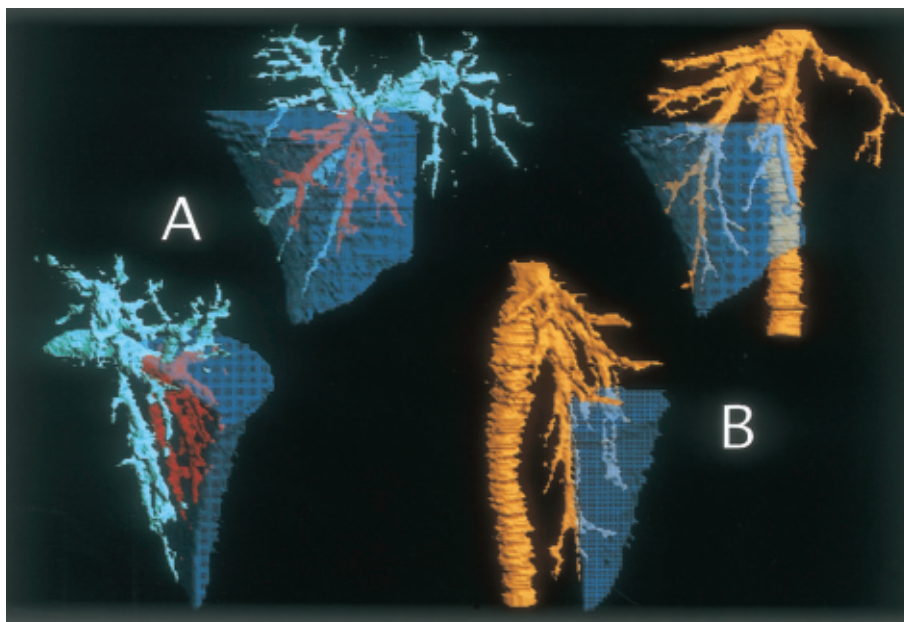
Fig. 3. Verification of blood vessel system (S5). The portal vein and the hepatic vein are different colors within the indicated subsegment. The volume of each subsegment is also stated. The volume of subsegment S5 is 219 ml (cm²). A : Portal vein system. B : Hepatic vein system.

acts as a drainage vessel can be assigned different colors to verify that the division of segments corresponds to anatomical divisions according to dominant blood vessels. Most incurrent blood vessels and drainage vessels were confirmed to be appropriately located in the segmental area (Fig. 3).

Simulation of hepatectomy

We investigated the use of segment identification in hepatectomy.

1. Resection of segment S8

First, we confirmed segment S8 with the system. The color of S8 was changed to one different from that of other parts of the hepatic surface (Fig. 4). To minimize blood loss and to ensure the proper amount of tissue was resected, the ideal procedure is to reach the Glisson's vessels that flows into S8, process them, then to resect the discolored area. In other words, the efficiency of surgery would be improved by identifying the point on the segmental borderline indicating the shortest route from the liver surface to the root of the Glisson's vessel and then dissecting the liver to the root from that point. In addition, the plane through which the root is reached is the segmen-

tal interface ; thus, only small, peripheral blood vessels would be cut and bleeding would be minimized.

Because this system can be used to measure distances, subsequent processing can be used. With this system, the point from which distances are being measured is yellow (Fig. 4). The distance from this point to the dorsal branch root was 35 mm, and the distance to the ventral branch root was 46 mm (Fig. 4B). If the portal vein is first processed and dissection is performed for these distances from this point, the lines demarcating segment S8 would be defined. Therefore, according to this line, the liver could be resected from the surface to the root that has been already processed. During the procedure, the only major requirement is that the hepatic vein is processed. During surgery, the problem is identifying 1) the point on the surface indicating the shortest distance and 2) the direction of the interface, but they can be approximated if landmarks on the hepatic surface are established (e.g., the most caudal point of the liver, the point 5 cm from the most-caudal point along the edge of the liver, and the boundary of the medial and lateral segments) and the distances from them are calculated (Fig. 4A).
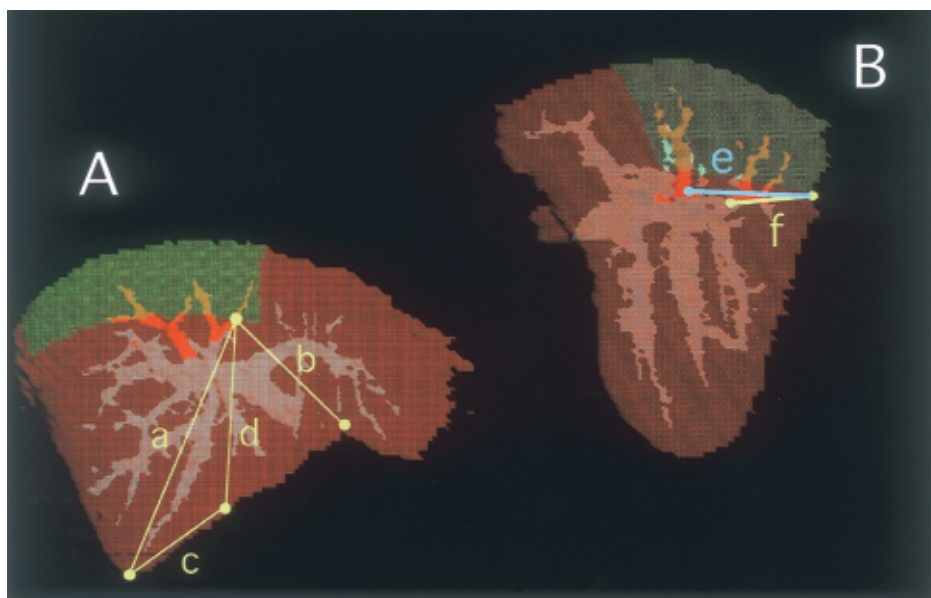
Fig. 4.   Simulation of S8 subsegmentectomy.   A : The shortest point to the root of S8 dominant portal vein on the surface and method to predict the shortest point.   a.   Distance from the most caudal point of the liver : 12 cm.   b.   Distance from the boundary point of the medial and lateral segments : 7 cm.   c.   Distance between the most caudal point and an optional point along the edge of the liver (in this figure, 5 cm).   d. Distance from the optional point along the edge of the liver : 8.5 cm.   B : The distance between point A and each root.   e.   The ventral branch root : 46 mm.   f.   The dorsal branch root : 35 mm.
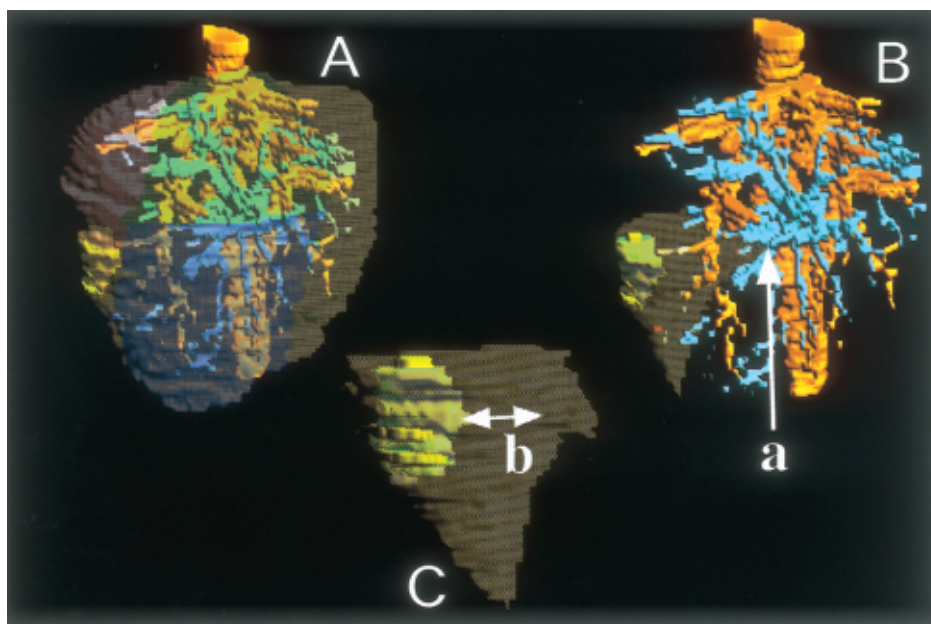
Fig. 5.   Resection of S6 subsegment in the patient with cancer.   3D image reconstructed from 4-mm-slice data. Portal vein : blue, Hepatic vein : orange, S5 : navy, S6 : dark yellow, S7 : purple, S8 : green, Tumor : yellow.   A : S6 subsegement containing the tumor.   B : Confirmation of the root of S6.   a.   Bifurcation of S6 and S7.   C : Resected sample to be predicted.   b.   33 mm.

2. Resection of segment S6

A simulation was performed on the basis of 3D images obtained from the patient with cancer. The positions of the Glisson's vessel to be processed and the point nearest to it on the surface could be predicted by displaying only the part (S6, in this case) to be
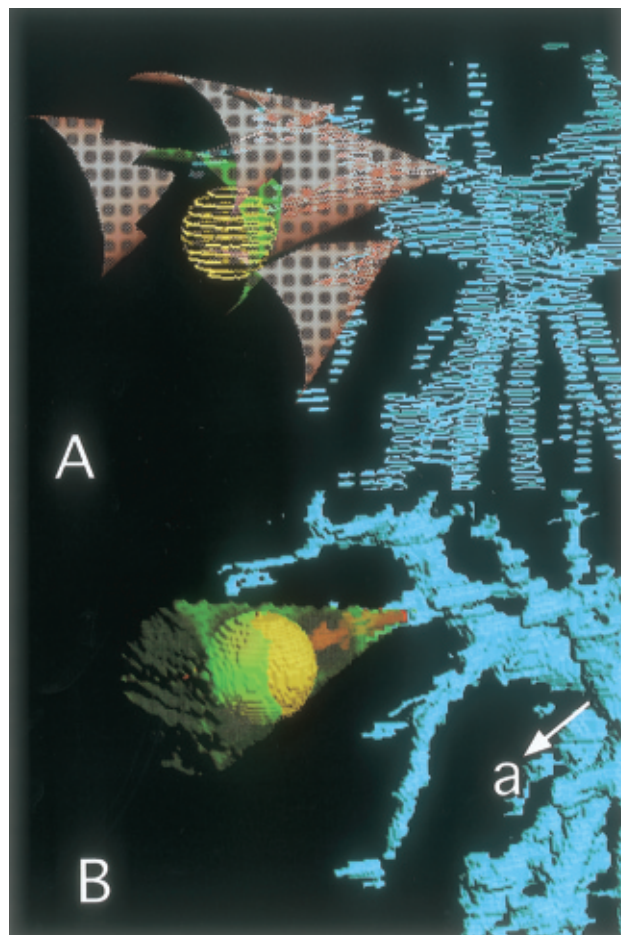
Fig. 6. Resection of smaller subsegment. A : Cone generated from the peripheral bifurcation of the portal vein that flowed into the tumor and cones generated from the circumferential portal ramification. B : Area to be resected surrounded by interface that divides the common area equally. a. root of S7.

resected (Fig. 5A, B). It might also be possible to observe theoretical resection margins (Fig. 5C) and to examine the appropriateness of operative procedures on the basis of volume measurements. Using this image, we determined that the volume of resection was 125.5 ml, the tumor volume was 20.6 ml, the hepatic resection rate was 11.4%, and the functional resection rate was 9.4%. The results showed that the quality of the 3D image made from the 4-mm-slice data was lower than that from 2-mm-slice data but was sufficient for practical operative simulation.

3. Resection of a smaller segment

We simulated the resection of a 20-mm-diameter tumor on the periphery of segment S7. From the peripheral bifurcation of the portal vein branch that supplied the tumor, we generated a cone containing the tumor. Interfaces with other cones could be generated from the circumferential portal ramification in the same way as the liver was divided into segments (Fig. 6). We could recognize the area surrounded by these interfaces as the smaller segment to be resected. In this case, we recognized one part of the tumor that could not be resected ; therefore, S7 segmentectomy or nonanatomic resection will be required.

DISCUSSION

Our system can be used to identify segments with minimal dissociation among the venous system, Glisson's system, and liver surface in the 3D space because all data are obtained from the same slices. Moreover, structures beneath the liver surface can be visualized and displayed separately or as standard 3D images. This feature should be useful for general surgeons to convert difficult hepatectomies to simpler procedures.

One reason why hepatectomy is difficult for general surgeons is that the volume of resection directly affects postoperative liver function. Malignant tumors of the hepatobiliary tract, such as hepatocellular carcinoma (HCC), metastatic hepatic tumors, and cholangiocellular carcinoma, can be treated surgically ; however, whether surgery is indicated and which procedure should be performed depend in part on the volume of resection and predicted remaining liver function. In patients with HCC, which usually arises from liver cirrhosis due to hepatitis B or C virus infection, the poor hepatic functional reserve requires various surgical techniques according to the tumor size and location. Lobectomy (major hepatectomy), a type of anatomic liver resection, should be the standard procedure for large HCCs ; however, HCCs are now often found when they are much smaller because of improvements in diagnostic imaging[16]. Accordingly, to maintain remnant liver function and not to

decrease curability, both small and large HCCs should be treated with anatomic segmentectomy based on the dominant portal vein[16]. The failure to perform suitable anatomic segmentectomy may allow portal invasion in many cases of small hepatic cancer[16]. Even when anatomical resection is not required, segmentectomy may be the most suitable method of resecting tumors in the deep liver parenchyma.

For such anatomic segmentectomy, the borders of the segment to be resected must be visualized on the liver surface. Makuuchi, et al. established a method for recognizing borders of a segment by infusing pigment into the segment's dominant portal vein identified on intraoperative ultrasound[16]. This method allows visualization of segmental borders that cannot be identified on the liver surface. However, surgeons may experience problems with intraoperative ultrasound, the complexity and incompleteness of dyeing, and failure of tattooing; therefore, segmentectomy requires specialized techniques. Additional problems that surgeons must overcome in hepatectomy include the difficulty of understanding intrahepatic anatomy (including Glisson's system and hepatic veins, which are within the liver parenchyma and cannot be seen from the liver surface) and the difficulty of controlling bleeding.

Recent developments in imaging diagnosis have enabled the 3D structure of intrahepatic vessels to be understood before surgery. However, imaging studies are usually done only to confirm the relationship between structural elements and the tumor and not to provide the surgeon with useful information during surgery. For this reason, we have developed a 3D system that can be used to identify segments during liver resection.

Several classifications of hepatic segments based on incurrent hepatic blood vessels have been reported[15,17]. Of these classifications, Couinaud's has become the most widely known. However, accurately defining segmental borders according to Couinaud's classification is so difficult that for convenience the borders for three segments of the right side of liver are established with planes that contain the inferior vena cava and each hepatic vein (middle and right). However, a discrepancy arises between the Couinaud's segment interface and the actual segmental interface based on the incurrent blood vessels because of the difference in position between the main portal trunk and the inferior vena cava. Furthermore, the rostral-caudal interfaces of segments cannot be determined in the absence of landmarks.

Our method for defining interfaces differs from previous methods. Rather than being based on anatomic landmarks, our method is based on incurrent blood vessels and their dominant areas, which are the basis for classifying liver segments. Because the dominant area of the incurrent blood vessel spreads radially along the vessels, we assumed the segment would be a cone whose apex was at the bifurcation of the vessels. In this trial, segments were defined by cones generated from the third ramifications of the main portal vein. However, by comparing segmented areas and the blood vessel system, we verified that each area contained the appropriate dominant portal vein up to the peripheral branch. Therefore, segments can be determined on the basis of incurrent vessels with cones generated from ramifications at this level. We believe that segmental borders on the liver surface determined with this system will correspond closely with the actual excisional planes. Thus, we believe our system of segmentation is more appropriate for clinical use.

Our system provides surgeons with further information on structures not visible on the liver surface so that the area to be resected can be defined without difficulties, such as those that can arise with staining. Methods such as the simulations described earlier can facilitate safe vessel exposure and decrease invasiveness and operating time. Furthermore, unnecessary resections might be prevented. In some patients with severe cirrhosis, extensive hepatectomy is contraindicated because of poor hepatic function. For such patients, our method can simulate smaller segmentectomy by defining smaller segments with cones generated from more-peripheral portal branches. Ideally, processing blood vessels based on the dominant portal vein might allow tumors to be completely removed without excess tissue resection.

Another feature of our system is that different structures (venous system, Glisson's system, liver sur-

face) are extracted from the same slices. As a result, all structures have a common coordinate axis and show no dissociation and simulation is more accurate. Our system should be useful for accurately measuring the distance between the liver surface and the vessel to be processed.

For operations based on hepatic functional reserve, predictions of anatomical excision range are not necessary, but predictions of the volume of liver parenchyma from which tumors are to be excised and of the remnant liver weight are essential[18]. In our system, on-image two-point distances and volumes of any segment or tumor can be measured by calculating the constituent voxels. Furthermore, any part of the 3D image can be resected and planes of resection can be observed from any direction. We believe that these functions of our system can be used to assess proposed procedures on the basis of functional reserve and to assess the predicted specimens.

We believe the accuracy of this system is high ; the error of measuring a phantom organ with our prototype system was less than 10%[8]. The error between the actual volume of an organ and the measured volume from CT images is estimated to be 5%[19]. Therefore, this system is sufficiently accurate for clinical use. For example, liver volume in a healthy man is 1,000 to 1,500 ml, and the ratio of the left lobe to the right lobe is usually 1 : 2[8,19]. With our system the liver volume of a healthy volunteer was 1,219 ml and the ratio of the left lobe to the right lobe was 1 : 1.83.

Our system provides information that is difficult to obtain with earlier types of 3D images and allows liver resection to be accurately simulated. This system can help hepatectomy to be performed safely and efficiently. We believe our system will allow liver resection to become a standard operation, even for general surgeons.

However, this system also has several limitations. The greatest limitation is the time needed to construct the 3D image because of difficulties in extracting vessels from two-dimensional slices. Because the computer has difficulty distinguishing vessels from noise in the liver parenchyma, part of this process must be performed manually. However, this process

can be improved by adjusting contrast conditions and the method of CT radiography and by eliminating noise with image-processing software. Furthermore, the procedure might be successfully automated by creating an algorithm that connects neighboring vessels on sequential slices. The accuracy of 3D images can be increased by obtaining a larger number of CT data slices of smaller pitch. However, in actual clinical practice, the pitch of slices and image accuracy are less than optimum owing to the cost and time of scanning, the dose and injection duration of contrast agents, and the duration of breath-holding. Improvements in scanning equipment might help solve such problems.

A second limitation of this system is that it cannot distinguish the caudate lobe. Even in clinical practice, the caudate lobe is difficult to define because the vessels corresponding to the segmental rami that are dominant in the caudate lobe are not large enough to be detected on CT images with current equipment. Furthermore, caudate lobe rami show numerous variations. However, if caudate lobe rami can be visualized with improved two-dimensional CT images, the caudal lobe can be distinguished in 3D imagery with our system.

Some recently developed 3D models can transform data and provide tactile feedback, and virtual reality-aided surgery is developing rapidly[12−14,20,21]. Our system might evolve into a four-dimensional system that can provide updated images in real time during surgery and project images on the liver surface to guide resection.

References

1. Brancatisano R, Isla A, Habib N. Is radical hepatic surgery safe ? Am J Surg 1998 ; 172 : 161-3.
2. Zoedler T, Ebener C, Becker H, Roeher HD. Evaluation of liver function tests to predict operative risk in liver surgery. HPB Surg 1995 ; 9 : 13-8.
3. Malassagne B, Cherqui D, Alon R, Brunetti F, Humeres R, Fagniez PL. Safety of selective vascular clamping for major hepatectomies. J Am Coll Surg 1998 ; 187 : 482-6.
4. Van Leeuwen MS, Noordzij J, Fernadez MA, Hennipman A, Feldberg MAM, Dillon EH. Portal venous and segmental anatomy of the right hemiliver : observation

based on three-dimensional spiral CT renderings. AJR 1994 ; 163 : 1395-404.

5. Kashiwagi T, Murakami T, Azuma M, Tamaki J, Ishibasi K, Kishida Y, et al. Three-dimensional display of liver, spleen, hepatoma, and blood vessls by MR imaging and computer graphics. Acta Radiol 1994 ; 35 : 88-9.

6. Evertsz CJG, Jürgens H, Peitgen HO, Berghorn W, Biel M, Breitenborn J, et al. Computer assisted problem-solving in radiology. Med Imag Tech 1996 ; 14 : 643-51.

7. Soyer P, Dufresne AC, Somveille E, Scherrer A. Focal nodular hyperplasia of the liver : assessment of hemodynamic and angioarchitectural patterns with gadolinium chelate-enhanced 3D spoiled gradient-recalled MRI and maximum intensity projection reformatted images. J Comput Assist Tomogr 1996 ; 20 : 898- 904.

8. Unemura Y, Suzuki N, Okamura T, Noda T, Sakurai K. Three-dimensional image of the liver in the perioperative period. Jikeikai Med J 1993 ; 40 : 139-49.

9. Takahashi S, Hattori A, Machida F, Uchiyama A, Suzuki N. Three- dimensional simulation of liver reproduction after hepatic lobectomy. Proceedings of the SPIE Vol. 1897 Image capture, formatting, and display ; 1993 Feb 14-15 ; Newport Beach, California, USA ; 1993. p. 99-107.

10. Hashimoto D, Dohi T, Tsuzuki M, Horiuchi T, Ohta Y, Chinzei K, et al. Development of a computer-aided surgery system : three-graphic reconstruction for treatment of liver cancer. Surgery 1991 ; 109 : 637-49.

11. Ivanov KD, Diacov CD. Three-dimensional endoluminal ultrasound. Dis Colon Rectum 1997 ; 40 : 47-50.

12. Suzuki N, Hattori A, Kai S, Ezumi T, Takatsu A. Surgical planning system for soft tissues using virtual reality. In : Medicine Meets Virtual Reality, Morgan KS et al, editors. IOS Press 1997. p. 159-63.

13. Suzuki N, Hattori A, Ezumi T, Uchiyama A, Kumano T, Ikemoto A, et al. Simulator for virtual surgery using deformable organ models And force feedback system. In : Medicine Meets Virtual Reality, Westwood JD, Hoffman HM, Stredney D, Weghorst SJ, editors. IOS Press and Ohmsha 1998. p. 227-33.

14. Suzuki N, Hattori A, Takatsu A, Kumano K, Ikemoto A, Adachi Y, et al. Virtual surgery system using deformable organ models and force feedback system with three fingers. In : MICCAI'98, Wells WM, Colchester A, Delp S, editors. Proceedings of the First International Conference. 1998 Oct. Cambridge, MA, USA 1998. p. 397-403.

15. Couinaud C. Le foie, études anatomiques et chirurgicales. Paris : Masson et Cie ; 1957.

16. Makuuchi M, Hasegawa H, Yamazaki S. Ultrasonically guided subsegmentectomy. Surg Gynecol Obstet 1985 ; 161 : 346-50

17. Healey JE, Schroy PC. Anatomy of the biliary ducts within the human liver. Arch Surg 1953 ; 66 : 559-616.

18. Stone HH, Long WD, Smith RB, Haynes CD. Physiologic considerations in major hepatic resections. Am J Surg 1969 ; 117 : 78-84.

19. Henderson JM, Heymsfield SB, Horowitz J, Kutner MH. Measurement of liver and spleen volume by computed tomography. Radiology 1981 ; 141 : 525-7

20. Marescaux J, Clément JM, Tassetti V, Koehl C, Cotin S, Russier Y, et al. Virtual reality applied to hepatic surgery simulation : The next revolution. Ann Surg 1998 ; 228 : 627-34.

21. Rosen JM, Soltanian H, Rodett RJ, Laub DR. Evolution of virtual reality from planning to performing surgery. IEEE Eng Med Biol Mag 1996 ; March/April : 16-22.